Block by Extracellular Divalent Cations of *Drosophila* Big Brain Channels Expressed in *Xenopus* Oocytes

Gina M. Yanochko* and Andrea J. Yool*†
*Program in Pharmacology and Toxicology and †Department of Pharmacology and Department of Physiology, College of Medicine, University of Arizona, Tucson, Arizona 85724

ABSTRACT *Drosophila* Big Brain (BIB) is a transmembrane protein encoded by the neurogenic gene *big brain* (*bib*), which is important for early development of the fly nervous system. BIB expressed in *Xenopus* oocytes is a monovalent cation channel modulated by tyrosine kinase signaling. Results here demonstrate that the BIB conductance shows voltage- and dose-dependent block by extracellular divalent cations Ca^{2+} and Ba^{2+} but not by Mg^{2+} in wild-type channels. Site-directed mutagenesis of negatively charged glutamate (Glu^{274}) and aspartate (Asp^{253}) residues had no effect on divalent cation block. However, mutation of a conserved glutamate at position 71 (Glu^{71}) in the first transmembrane domain (M1) altered channel properties. Mutation of Glu^{71} to Asp introduced a new sensitivity to block by extracellular Mg^{2+}; substitutions with asparagine or glutamine decreased whole-cell conductance; and substitution with lysine compromised plasma membrane expression. Block by divalent cations is important in other ion channels for voltage-dependent function, enhanced signal resolution, and feedback regulation. Our data show that the wild-type BIB conductance is attenuated by external Ca^{2+}, suggesting that endogenous divalent cation block might be relevant for enhancing signal resolution or voltage dependence for the native signaling process in neuronal cell fate determination.

INTRODUCTION

The neurogenic gene *big brain* (*bib*) encodes the transmembrane channel protein, Big Brain (BIB). BIB is a member of the Major Intrinsic Protein (MIP) family (Rao et al., 1990) that includes mammalian Aquaporin-1 (AQP1), known to mediate osmotic water flux (Preston et al., 1992) and function as a gated ion channel (Anthony et al., 2000; Yool et al., 1996). The carboxyl terminal domain of BIB diverges substantially in length and complexity from those of other members of the MIP family and carries a number of potential regulatory domains for protein-protein interactions and serine/threonine and tyrosine phosphorylation (Yanochko and Yool, 2002). Expression of BIB in *Xenopus* oocytes does not induce osmotic water permeability, but does confer a novel monovalent cation conductance that is activated in response to endogenous oocyte signaling pathways and modulated by tyrosine kinase (Yanochko and Yool, 2002).

In the fly, loss-of-function mutations in the *big brain* gene cause an approximately twofold increase in the number of neuroblasts formed during *Drosophila* neurogenesis by impairing the process of lateral inhibition. Loss-of-function mutations in other neurogenic genes such as *Notch* or *Delta* have a similar but more severe phenotype (Lehmann et al., 1983; Rao et al., 1992). The *bib* gene is expressed in epidermal cells and acts cell autonomously to maintain an epidermal fate and inhibit the neural fate. Its synergistic interaction with *Notch* and *Delta* suggested that BIB is involved in mediating the response to the lateral inhibition signal (Doherty et al., 1997).

A high amino acid sequence identity (40%) in the transmembrane domains between BIB and the lens MIP ion channel (AQP0) supported the hypothesis that BIB functions as an ion channel (Rao et al., 1990), but its putative channel properties remained uncertain until a regulated ionic conductance was described (Yanochko and Yool, 2002). The intracellular linker between transmembrane domains M1 and M2 (loop B) and the extracellular linker between M5 and M6 (loop E) contain the hallmark sequence of the MIP family, an asparagine-proline-alanine (N-P-A) motif. Of particular interest for our study is that a conserved glutamate in M1 (Glu^{71} of BIB) is present in more than 90% of MIP channels (Reizer et al., 1993), suggesting an important role for this residue in maintaining channel structure and function.

Previous work (Yanochko and Yool, 2002) demonstrated that the process of spontaneous activation in BIB-expressing oocytes was initiated by the pricking effect of electrode insertion by unidentified endogenous signaling pathways and was not affected by holding potential or voltage steps or by placing oocytes into recording saline for equivalent time periods. The current began to activate ~5 min after electrode insertion and reached a plateau at ~20–30 min after electrode insertion. The response was reversible; oocytes recovered to initial low conductance levels when tested after ~4 h or more of rest. Western blot analysis confirmed that BIB protein was tyrosine phosphorylated. The conductance response was decreased after treatment with 20 μM insulin and enhanced by 10 μM lavendustin A, a tyrosine kinase inhibitor. Both tyrosine phosphorylation and the potentiating effect of lavendustin A were removed by partial deletion of the carboxy terminal (aa 317–700). Current activation was

Submitted July 16, 2003, and accepted for publication October 30, 2003.

Address reprint requests to Andrea J. Yool, Dept. of Physiology, PO Box 245051, University of Arizona, Tucson, AZ 85724-5051. Tel.: 520-626-2198; Fax: 520-626-2383; E-mail: ayool@u.arizona.edu.

Gina M. Yanochko's present address is Molecular and Cell Biology Laboratory, The Salk Institute for Biological Studies, La Jolla, CA 92037.

0006-3495/04/03/1470/09 $2.00

not observed in control oocytes or in oocytes expressing a nonfunctional mutant (BIB E71N) that appeared to be expressed on the plasma membrane, as determined by confocal microscopy and Western blotting. These results showed that the activation of BIB channels may involve tyrosine kinase-mediated signaling (Yanochko and Yool, 2002).

With the goal of further characterizing the properties of BIB ion channels, we investigated the effects of extracellular Ca^{2+}, Ba^{2+}, and Mg^{2+}. The observation of divalent cation block is novel for BIB channels, but equivalent phenomena serve important physiological roles in other ion channels, including for example light adaptation of the response mediated by cyclic-GMP-gated channels in rod photoreceptors (Kaupp and Seifert, 2002), voltage dependence of inwardly rectifying K^+ channels in neuronal and cardiac cells (Nichols and Lopatin, 1997), the combined depolarization- and glutamate-dependent activation of *N*-methyl-D-aspartate receptors in neuronal postsynaptic membranes (MacDonald and Nowak, 1990), and others.

The contribution of negatively charged amino acids to divalent cation block in BIB was tested with site-directed mutagenesis of Glu^{71}, Asp^{253}, and Glu^{274} of BIB. Mutation of Asp^{253} or Glu^{274} to asparagine had little effect on whole-cell conductance as compared to wild type and did not alter the block by divalent cations. However, substitution of BIB Glu^{71} with asparagine, glutamine, lysine, or aspartate (E71N, E71Q, E71K, and E71D) differentially affected whole-cell conductance and plasma membrane protein expression. The conservative mutation of Glu^{71} to Asp (maintaining a negative charge while decreasing side-chain size) induced a novel sensitivity to block by extracellular Mg^{2+} in BIB E71D-expressing oocytes. Two other substitutions (E71N and E71Q) virtually eliminated ionic conductance without preventing protein trafficking to the plasma membrane. The switch from a negative to a positive side-chain charge (E71K) appeared to disrupt proper channel assembly or membrane targeting, resulting in a loss of measurable protein expression in the membrane.

Our results are the first to show divalent channel block of BIB channels and to identify a critical role for the conserved amino acid Glu^{71} in influencing the pore properties of a MIP channel. Our mutagenesis studies suggest the contribution of Glu^{71} depends critically on both side-chain charge and size. These data support the idea that the conserved Glu residue in M1 is essential for divalent cation binding, either directly or indirectly by maintaining the positions of other residues that determine the structure of the ion channel pore. Crystal structures solved for other MIP channels predict that this Glu residue might interact indirectly with pore domain residues as a structural anchor. However, MIP channels have not yet been imaged in a demonstrated open (ion conducting) state, so the alternative possibility that there are conformational changes during channel opening that reposition the Glu^{71} residue cannot be ruled out. Distinguishing these possibilities awaits structure imaging studies of MIP channels in the presence of identified ion channel activators.

MATERIALS AND METHODS

Molecular techniques

Cloned cDNA for wild-type *Drosophila* BIB was kindly provided by Drs. L. and Y. N. Jan (Rao et al., 1990). The BIB cDNA construct used to generate wild-type and mutant channels was modified by the addition of a hemagglutanin epitope tag to the amino terminal that does not interfere with channel function (Yanochko and Yool, 2002). Site-directed mutagenesis was performed on BIB constructs in the *Xenopus* β-globin expression vector (p$X\beta$Gev) with the Stratagene QuikChange site-directed mutagenesis kit (Stratagene, La Jolla, CA). Asp^{253}, Glu^{274}, and Glu^{71} were mutated to asparagine (D253N, E274N, and E71N). Glu^{71} was also mutated to lysine (E71K), glutamine (E71Q), and aspartic acid (E71D) using the following primer combinations (mutated bases underlined):

D253N
sense: 5′-GTGCTTAACAAATGG**A**ACAGCCATTGGGTGTACTGG-3′ (bp 1042-1077)
antisense: 5′-CCAGTACACCCAATGGCTGT**T**CCATTTGTTAAG-CAC-3′ (bp 1077-1042)
E274N
sense: 5′-GGCCTGGTGTAC**A**A**C**TACATCTTCAACTCGCGC-3′ (bp 1108-1140)
antisense: 5′-GCGCGAGTTGAAGATGTA**G**T**T**GTACACCAGGCC-3′ (bp 1140-1108)
E71N
sense: 5′-GGAGATCCATCATCAGC**A**A**C**TGTCTGGCCTCC-3′ (bp 494-525)
antisense: 5′-GGAGGCCAGACA**G**T**T**GCTGATGATGGATCTCC-3′ (bp 525-494)
E71K
sense: 5′-GGAGATCCATCATCAGC**A**AGTGTCTGGCCTC-3′ (bp 494-524)
antisense: 5′-GAGGCCAGACACT**T**GCTGATCATCGATCTCC-3′ (bp 524-494)
E71Q
sense: 5′-GGAGATCCATCATCAGC**C**AGTGTCTGGCCTC-3′ (bp 494-524)
antisense: 5′-GAGGCCAGACACT**G**GCTGATGATGGATCTCC-3′ (bp 524-494)
E71D
sense: 5′-CCATCATCAGCGA**C**TGTCTGGCCTCCTTC-3′ (bp 500-528)
antisense: 5′-GAAGGAGGCCAGACA**G**TCGCTGATGATGG-3′ (bp 528-500).

The entire coding sequences of all constructs were sequenced to verify that no additional mutations were introduced by polymerase error. Plasmid DNA was linearized with *Spe*I in the polylinker region and used to transcribe RNA in vitro with T3 RNA polymerase. Enzymes were purchased from Roche Molecular Biochemicals (Indianapolis, IN).

Oocyte preparation and injection

Stage V-VI oocytes from adult female *Xenopus laevis* were obtained and defolliculated as described by Anthony et al. (2000). Prepared oocytes were injected with 50 nl sterile water (control oocytes) or 50 nl sterile water containing *bib* or mutated *bib* cRNA (20 ng) and were incubated for 2–5 days at 18°C in ND96 culture medium (96 mM NaCl, 2 mM KCl, 1.8 mM $CaCl_2$, 1 mM $MgCl_2$, 5 mM Hepes, 2.5 mM pyruvic acid, 100 units/ml penicillin, and 100 μg/ml streptomycin, pH 7.6) to allow protein expression before recording.

Electrophysiological recordings

Two-electrode voltage clamp was used to investigate the macroscopic ion channel properties of BIB. Recordings were performed at room temperature with electrodes (0.5–3 MΩ) filled with 3 M KCl. Data were recorded with a GeneClamp 500 (Axon Instruments, Foster City, CA), filtered at 1 kHz, and analyzed with pClamp software (Axon Instruments). Standard recording saline for two-electrode voltage clamp contained (in mM): 100 NaCl, 2 KCl, 4.5 $MgCl_2$, 2 EGTA, 5 Hepes, pH 7.3. Free Ca^{2+} and Ba^{2+} concentrations were calculated by MaxChelator (http://www.stanford.edu/cpatton/maxc.html). Reversal potentials were obtained from model-independent second-order polynomial fits of the current-voltage relationships for each oocyte.

The effects of divalent cations (Ca^{2+} and Ba^{2+}) were tested by perfusion of modified salines in which $MgCl_2$ was partially or fully substituted with $CaCl_2$ or $BaCl_2$. In a subset of experiments used to test for chronic block of E71D channels, the standard Mg^{2+} saline contained 100 mM NaCl, 5 mM $MgCl_2$, and 10 mM Hepes, pH 7.3; and the low Mg^{2+} saline contained 106 mM NaCl, 0.5 mM $MgCl_2$, and 10 mM Hepes, pH 7.3. Channel activation was monitored by repeated steps to +40 mV (800-ms duration) every 5 s from a holding potential of −40mV as previously described (Yanochko and Yool, 2002). Conductance was measured as the slope of a linear fit of the current-voltage relationship between +40 and −70 mV. The *% block* was calculated as $[(Go - Gx)/Go] \times 100$ where *Go* was the conductance measured in standard recording saline with Mg^{2+}, and *Gx* was the conductance measured in the test saline with the substituted divalent cation *x*. The magnitude of the relative outward rectification was calculated from the absolute value of the ratio of current amplitudes measured at two points, +50 and −70 mV, selected as being approximately equidistant from the reversal potential (−17 mV). A ratio of 1.0 indicates a linear current-voltage relationship, >1 indicates outward rectification, and <1 indicates inward rectification.

Cellular fractionation

A total of 2–3 days after RNA injection, oocyte plasma membranes were isolated as previously described (Yanochko and Yool, 2002). Pellets enriched in plasma membrane proteins were resuspended in 25 μl Laemmli buffer (10% glycerol, 50 mM Tris HCl, 2% sodium dodecyl sulfate (SDS), 5% β-mercaptoethanol, 0.02% bromophenol blue) and resolved by SDS-polyacrylamide gel electrophoresis for Western blotting.

Western blotting

Proteins resolved by 10% SDS-polyacrylamide gel electrophoresis were transferred to polyvinylidene difluoride (PVDF) membrane supports (Bio-Rad, Hercules, CA) in transfer buffer (10% methanol, 10 mM 3-(cyclohexylamino)-1-propanesulfonic acid (CAPS); Sigma, St. Louis, MO) for 1 h at 1 Å. Nonspecific binding sites were blocked with 1.5% (w/v) evaporated milk in TBST (154 mM NaCl, 10 mM Tris-base, 0.2% Tween-20), 0.01% thimerosal for 1 h at room temperature, or overnight at 4°C. After blocking the blot was incubated for 1 h at room temperature with the primary antibody (rat anti-hemagglutanin antibody clone 3F10, 50 ng/ml; Roche) followed by three washes in TBST. Immunoreactive bands were visualized by enhanced chemiluminescence (Pierce, Rockford, IL) with horseradish peroxidase-conjugated goat anti-rat secondary antibody (0.25 μg/ml; Zymed Laboratories, San Francisco, CA).

All data summaries are reported as mean ± SD, unless otherwise noted. Statistical significance was determined with a two-tailed Student's *t*-test or one-way analysis of variance (ANOVA) with Bonferroni post-hoc test, where indicated; $p < 0.05$ was used to determine significance.

RESULTS

The blocking effects of $CaCl_2$ and $BaCl_2$ on the BIB ionic current are shown in Fig. 1. BIB channels are activated by an endogenous signaling cascade in *Xenopus* oocytes that is triggered by pricking (electrode penetration) and modulated by tyrosine kinases (Yanochko and Yool, 2002). BIB channel activation as a function of time after electrode penetration was monitored with repeated steps to +40 mV from a holding potential of −40 mV. After full activation in standard Mg^{2+} saline, saline containing 4.5 mM Ca^{2+} or Ba^{2+} substituted for Mg^{2+} was perfused into the recording chamber (five times the bath volume delivered in <15 s). The rapid subsequent block of current is plotted in Fig. 1 *A*. Fig. 1 *B* shows representative traces of currents recorded from wild-type BIB-expressing oocytes in Mg^{2+}, Ca^{2+}, or Ba^{2+} salines and illustrates outward rectification with Ca^{2+} or Ba^{2+}. The divalent block of the wild-type BIB conductance was dose-dependent (Fig. 1 *C*). The log-linear plots of the percent block of conductance as a function of divalent cation concentration (*D*) were fit with the equation: $\%\ block = (D \times B_{max})/(D + IC_{50})$. Fits yielded estimated IC_{50} values (dose for 50% inhibition) of 4 μM for Ca^{2+} and 0.4 mM for Ba^{2+} (with *R* correlation coefficients of 0.93 and 0.91, respectively), and maximal % block (B_{max}) values of ~70% for Ca^{2+} and ~60% for Ba^{2+}. Fig. 1 *D* illustrates current-voltage relationships for the oocytes shown in Fig. 1 *B*. Reversal potentials in salines with Mg^{2+} (−17 ± 5 mV, $n = 14$), Ca^{2+} (−18 ± 9 mV, $n = 6$), and Ba^{2+} (−16 ± 5 mV, $n = 13$) were not significantly different.

Wild-type BIB channels have an approximately linear current-voltage relationship in Mg^{2+} saline and show outward rectification in Ca^{2+} and Ba^{2+} salines, suggesting that there is voltage-dependent unblocking by Ca^{2+} and Ba^{2+} at depolarized membrane potentials. We quantified the relative outward rectification by calculating the absolute value of the ratio of the current amplitudes measured at +50 and −70 mV. With comparable driving forces at these two voltages, linear current-voltage relationships yield relative outward rectification values of ~1.0. Fig. 1 *E* shows compiled data for the current ratios (I_{+50}/I_{-70}) for wild-type BIB channels in 4.5 mM Mg^{2+}, Ca^{2+}, or Ba^{2+} salines. The current ratio in Mg^{2+} was 1.5 ± 0.4 ($n = 30$). In Ca^{2+} saline, the magnitude of outward rectification (3 ± 3; $n = 15$) was significantly greater than in Mg^{2+} ($p < 0.01$; ANOVA, Bonferroni post-hoc test). Similarly, the outward rectification in Ba^{2+} saline (4 ± 1; $n = 30$; $p < 0.001$) was significantly greater than in Mg^{2+} saline. The magnitudes of relative outward rectification were not significantly different between the Ca^{2+} and Ba^{2+} salines for wild-type BIB channels.

Divalent cation block of ion channels is affected by negatively charged amino acids in pore lining regions (Park and MacKinnon, 1995). In BIB, two negatively charged amino acids (Asp^{253} and Glu^{274}) are located in the third extracellular loop (*loop E*) or flanking transmembrane domain M6 (Fig. 2 *A*), and none are in the first intracellular loop (*loop B*). Because loops B and E are known from crystal structures to contribute to the water and solute permeation

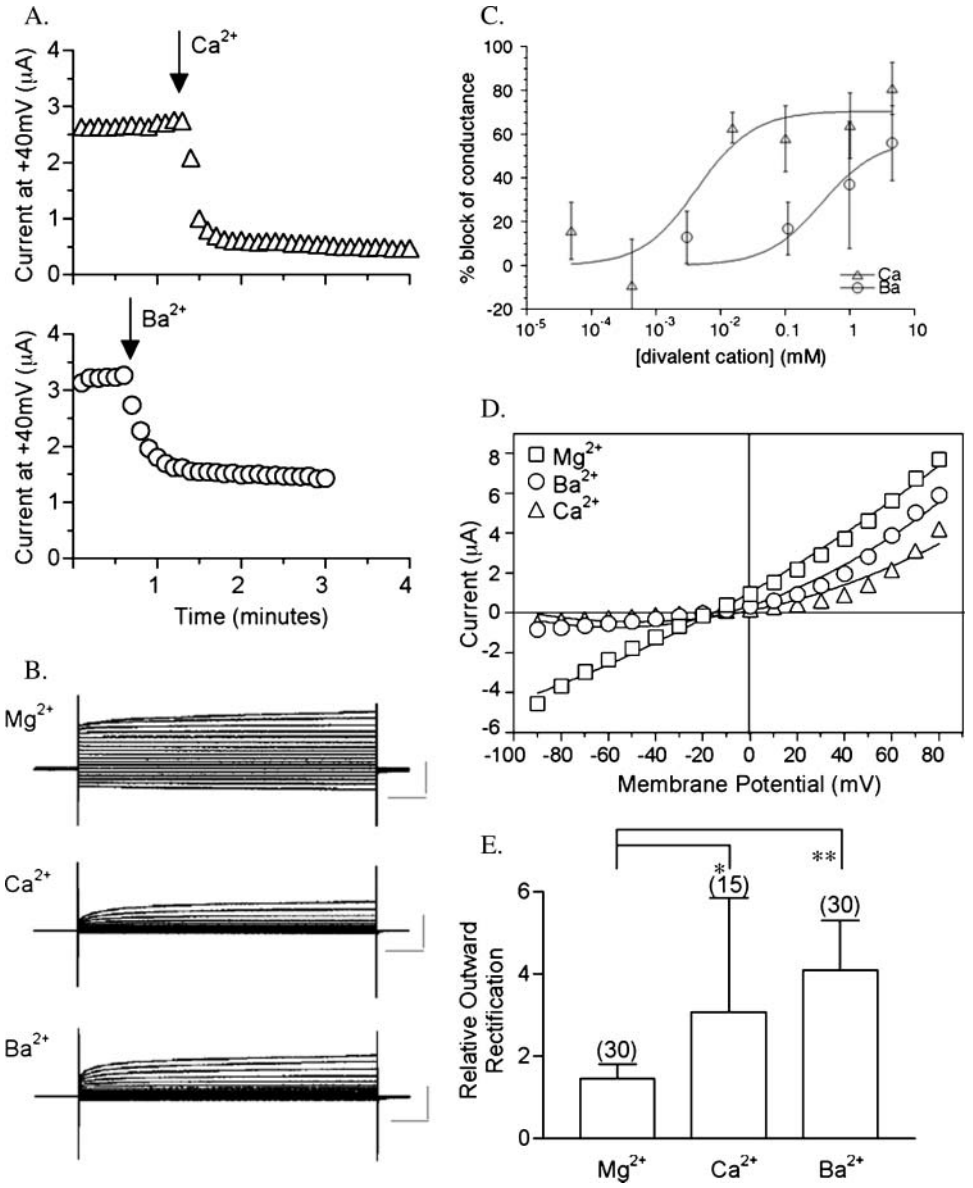

FIGURE 1 Block of wild-type BIB ionic current by extracellular calcium and barium. (*A*) Decrease in current amplitude after replacement of 4.5 mM Mg^{2+} saline with 4.5mM $CaCl_2$ or $BaCl_2$ saline, as monitored with repeated steps to +40 mV. (*B*) Representative current traces from +80 to −70 mV in 10-mV increments from a holding potential of −40 mV for wild-type BIB activated in Mg^{2+} saline and after perfusion with Ca^{2+} or Ba^{2+} salines. Scale bars indicate 5 μA and 100 ms. (*C*) Dose-dependent block of BIB conductance by external Ca^{2+} and Ba^{2+} (see text for details). Data points are mean ± SD, n = 3–12 per treatment. (*D*) Current-voltage relationships for data illustrated in *B*. (*E*) Summary histogram of the relative outward rectification values for wild-type BIB currents in salines containing 4.5 mM Mg^{2+}, 4.5 mM Ca^{2+}, or 4.5 mM Ba^{2+}. Rectification values are absolute values of the ratio of current magnitudes at +50 and −70 mV (see text for details). Asterisks indicate significance ($*p < 0.01$, $**p < 0.001$, ANOVA, Bonferroni post hoc test).

pathways in other MIP channels such as AQP1 and *Escherichia coli* glycerol facilitator (GlpF) (Fu et al., 2000; Sui et al., 2001), Asp^{253} and Glu^{274} were targeted for mutagenesis. Because of its conserved nature across MIP channels, Glu^{71} in the first transmembrane domain was also chosen as a site for mutagenesis. The BIB mutants D253N, E274N, E71N, E71Q, E71K, and E71D were generated and expressed in *Xenopus* oocytes for analyses of effects of divalent cations by two-electrode voltage clamp.

Fig. 2 *B* summarizes the macroscopic conductance responses of oocytes expressing BIB wild-type and mutant channels and control (water-injected) oocytes in standard recording saline. Data are organized to compare BIB and control responses from within the same batches of oocytes. The wild-type BIB conductance responses were 30 ± 22 μS ($n = 19$), 47 ± 30 μS ($n = 13$), and 36 ± 22 μS ($n = 12$) in the left, middle, and right panels respectively. Whole-cell conductances for E274N (35 ± 18 μS, $n = 19$) and D253N-expressing oocytes (21 ± 13 μS, $n = 21$) were not significantly different than those for wild-type BIB. In D253N and E274N BIB channels, the dose-dependent block by Ca^{2+} and the relative permeability values for K^+, Na^+, and TEA^+ were not different from those of wild type (data not shown).

At position 71, the conservative mutation of Glu to Asp showed a conductance response (6 ± 4 μS, $n = 11$) that was significantly less than wild type ($p < 0.01$), but significantly greater than control (1 ± 1 μS, $n = 6$, $p < 0.05$). In contrast, other mutations at this site were not well tolerated. Oocytes expressing E71N (6 ± 5 μS, $n = 17$), E71Q (0 ± 2 μS, $n = 3$), or E71K (0.4 ± 0.3 μS, $n = 3$) were not significantly different from control oocytes (4 ± 4 μS, $n = 7$). The lack of

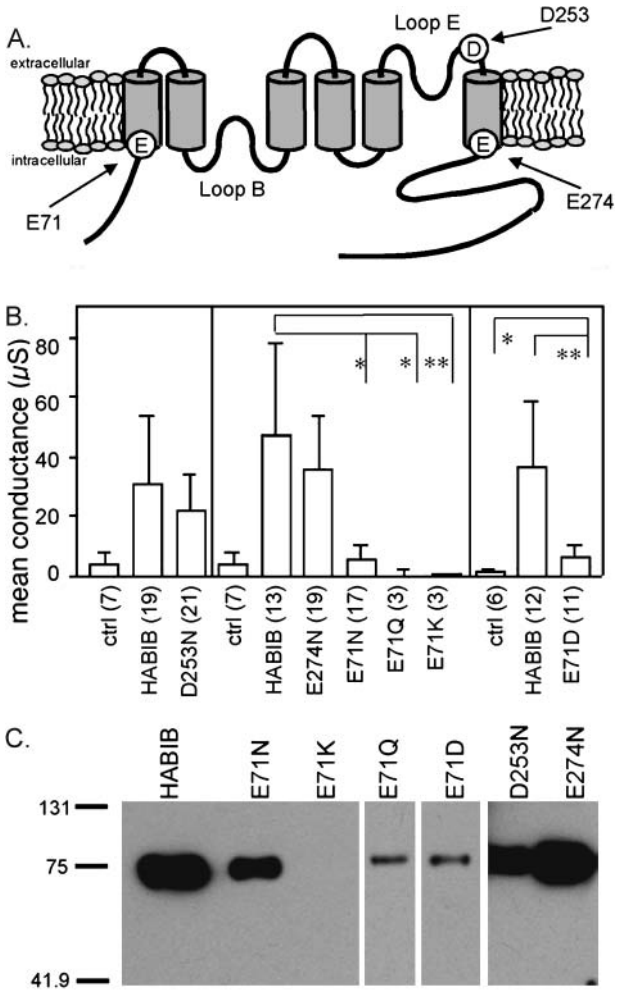

FIGURE 2 Effects of mutations D253N, E274N, E71N, E71Q, E71K, and E71D on BIB ionic conductance and plasma membrane expression. (*A*) Diagram of the likely transmembrane topology of BIB with six transmembrane domains and intracellular amino and carboxy termini. Sites of mutations are indicated by arrows. (*B*) Summary histogram showing the mean net conductance values for control oocytes and oocytes expressing wild-type and mutant BIB channels. Conductance was determined from linear fit of the current-voltage relationship between +40 and −70 mV; net conductances are final minus initial values. Control, mutant, and wild-type BIB data were compared within the same batches of oocytes (separated by *vertical lines*). Oocytes expressing D253N or E274N had net conductance values not significantly different from wild-type BIB. E71N (**$p < 0.01$), E71Q (*$p < 0.05$), and E71K (*$p < 0.05$) were significantly different from wild-type BIB but not from control. E71D also had significantly reduced net conductance (**$p < 0.01$) as compared to wild-type BIB but was significantly greater than control (*$p < 0.05$). (*C*) Western blot analysis of plasma membrane-enriched oocyte fractions showing the relative expression of BIB wild-type, D253N, E274N, E71N, E71Q, E71K, and E71D channels, but not E71K. Probing with rat anti-hemagglutanin antibody (3F10; Roche) for the epitope tag resolved BIB wild-type and mutant protein at the expected size of 80kD. No immunoreactive bands were seen from control oocytes (Yanochko and Yool, 2002).

an ionic conductance response in mutant channels could result from a direct effect on a functionally critical residue or indirectly from disruption of assembly or targeting. Trafficking to the plasma membrane for BIB mutant channels was tested by Western blot analysis of fractions enriched for oocyte plasma membrane proteins (Fig. 2 *C*). Wild-type channels and mutant D253N, E274N and E71N, E71Q, and E71D channels were identified at the expected size of ~80 kD, indicating that these constructs were expressed in plasma membrane although not necessarily with comparable efficiency. E71D channels were expressed in plasma membrane at a reduced level, which may explain in part the lower levels of whole-cell conductance that were observed. Switching the charge from negative to positive in E71K resulted in an absence of detectable protein in plasma membrane preparations and no ionic current, suggesting disrupted targeting or assembly of these mutant channels. The E71Q and E71N mutants were expressed in membrane but showed no appreciable ionic conductance, suggesting that the introduction of an uncharged polar residue at this position is not compatible with ion channel function in BIB.

The sensitivity of the BIB mutant channels to block by extracellular divalent cations was evaluated by comparing the magnitude of rectification in Mg^{2+}, Ca^{2+}, and Ba^{2+} salines (Fig. 3). Fig. 3 *A* shows representative current traces for voltage-clamped oocytes expressing BIB D253N, E274N, and E71D in Mg^{2+}, Ca^{2+}, and Ba^{2+} salines. Corresponding plots of the current-voltage relationships, each standardized to the current at +80 mV, are shown in Fig. 3 *B*. There was no discernable effect of the mutations at D253 or E274 as compared to wild type on the relative outward rectification induced by divalent cations. As shown in Fig. 4, the mean relative outward rectification values for D253N channels in saline with Mg^{2+} (1.4 ± 0.4, $n = 10$), Ca^{2+} (3 ± 1, $n = 9$), and Ba^{2+} (3 ± 1, $n = 11$) were not significantly different from those of wild-type BIB channels (Fig. 1 *E*). The outward rectification in Mg^{2+} saline was significantly less than that in Ca^{2+} ($p < 0.001$) or Ba^{2+} ($p < 0.01$) salines. E274N also showed relative rectification values in Mg^{2+} (1.5 ± 0.4, $n = 6$), Ca^{2+} (2 ± 1, $n = 6$), and Ba^{2+} salines (3.6 ± 0.8, $n = 12$) that were not significantly different from wild type.

In contrast, the mutation of E71D did alter divalent cation block as compared to wild type; the mutant channels gained sensitivity to block by Mg^{2+} (Figs. 3 and 4). For E71D, the magnitudes of outward rectification were comparable in all three salines: Mg^{2+} 2.3 ± 0.9 ($n = 17$), Ba^{2+} 2.9 ± 0.6 ($n = 7$), and Ca^{2+} 2.9 ± 0.2 ($n = 3$), and not significantly different from each other. E71D-expressing oocytes had significantly greater outward rectification in Mg^{2+} saline than did wild type ($p < 0.001$), whereas the rectification for E71D in Ca^{2+} or Ba^{2+} was not significantly different from that of wild type. The voltage-dependence of the blocking effect in the wild-type and mutant channels indicates that the divalent cation binding site is located within the electrical field, such as in the ion permeation pathway, rather than on the protein external surface. The effects of the mutations indicate that E71, but not D253 or E274, is located in a region that affects the divalent cation binding site.

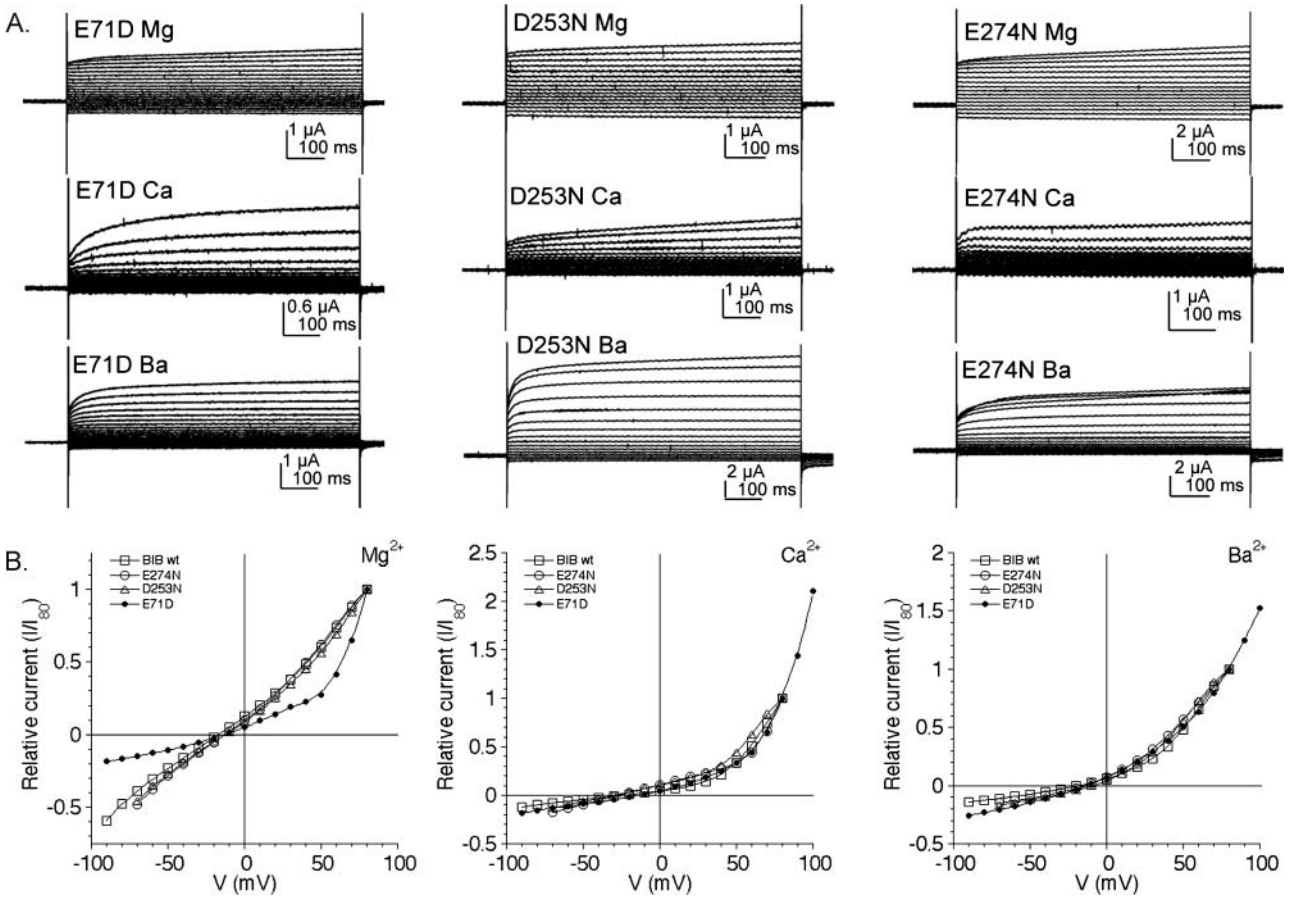

FIGURE 3 Divalent cation effects on outward current rectification for BIB E71D, D253N, and E274N mutant channels. (*A*) Current traces for D253N, E274N, and E71D BIB-expressing oocytes, measured from +80 to −70 mV in 10-mV increments from a holding potential of −40mV, in salines with 4.5 mM Mg^{2+}, Ca^{2+}, or Ba^{2+}. (*B*) Standardized current-voltage relationships for the traces illustrated in *A*, with currents referenced to the current amplitude measured at +80 mV (I/I_{+80}).

The Mg^{2+} block of E71D channels suggested that the low conductance observed for this construct might not be due only to decreased protein targeting, but might also reflect chronic channel block in the standard saline condition. Data compiled in Fig. 5 show that Mg^{2+} present in standard saline decreases the E71D channel conductance as compared with the response in 0.5 mM Mg^{2+}. Wild-type and E71D BIB currents were activated in standard Mg^{2+} saline (5 mM) and in low Mg^{2+} (0.5 mM) made isotonic with additional NaCl. For wild-type BIB, no significant difference in conductance amplitude was observed in 5 mM Mg^{2+} (78 ± 9.5 μS, mean ± SE, $n = 16$) as compared with 0.5 mM Mg^{2+} (71 ± 12 μS; mean ± SE, $n = 7$), showing that Mg^{2+} did not cause a discernable chronic block and confirming that standard Mg^{2+} saline is appropriate for analyses of wild-type BIB channels. In contrast, the conductance activated in E71D BIB-expressing oocytes in low Mg^{2+} saline (11 ± 3.4 μS, mean ± SE, $n = 9$) was approximately threefold greater than that in 5 mM Mg (3.5 ± 0.6 μS, mean ± SE, $n = 10$). Fig. 6 illustrates channel activation for a E71D-expressing oocyte that showed particularly poor activation in 5 mM Mg^{2+} saline; then after 3 h recovery in ND96 saline, the same oocyte showed a robust activation in 0.5 mM Mg^{2+}. These data support the conclusion that the mutation E71D alters the

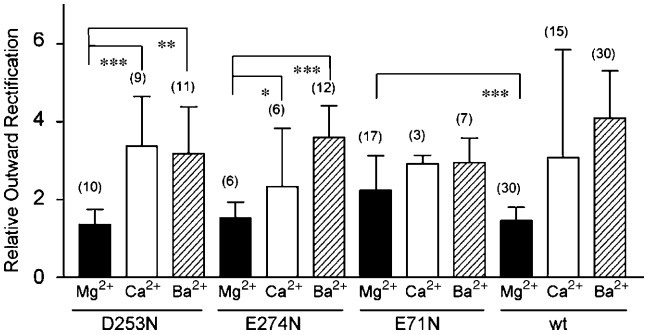

FIGURE 4 Summary histogram of the mean relative outward rectification values for BIB mutant channels. Compiled data for the relative outward rectification, measured as the ratio of current amplitudes at +50 and −70 mV, in salines with Mg^{2+} (*solid*), Ca^{2+} (*open*), or Ba^{2+} (*cross-hatched*). Statistically significant differences are shown as $^{***}p < 0.001$, $^{**}p < 0.01$, and $^{*}p < 0.05$. *n*-values are shown in parentheses; see text for summary data.

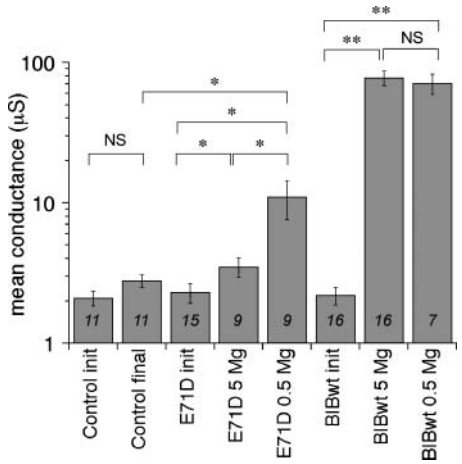

FIGURE 5 Summary histogram of BIB wild-type and E71D net conductance levels in standard and low Mg^{2+} salines. Statistically significant differences are shown as $^{**}p < 0.001$ and $^{*}p < 0.05$. *n*-values are shown on the histogram; see text for summary data.

BIB channel in a way that increases the affinity of a divalent cation binding site for Mg^{2+}. Thus, the reduced amplitude of the maximal conductance response of the E71D channel is attributable to chronic block by Mg^{2+}, as well as reduced protein expression in the plasma membrane.

DISCUSSION

Results here show that Big Brain monovalent cation channels expressed in *Xenopus* oocytes are blocked by extracellular divalent cations Ca^{2+} and Ba^{2+} but not Mg^{2+} in wild-type channels. Block by divalent cations is important in many types of channels for generating voltage-dependent function, enhancing signal resolution, and enabling feedback regulation. For example, in rod photoreceptors, block by divalent cations has been suggested to serve as an intracellular messenger system that controls physiological responses of ion channels to cGMP (Stern et al., 1987). External Ca^{2+} blocks the inward current of the rod cGMP-gated channel at micromolar concentrations in a voltage-dependent manner. Voltage-dependent block by divalent cations decreases the amplitude of rod single channel currents and has been suggested to reduce noise in the dark state and allow for single photon detection (Zimmerman and Baylor, 1992). A Glu residue in the pore region between transmembrane regions 4 and 5 in rod CNG channels appears to be an important determinant of Ca^{2+} affinity. The substitution of Glu with Asp enhances the affinity of Ca^{2+} binding (Kaupp and Seifert, 2002). These various studies show interesting parallels with our study of BIB channels in that substitution of Glu with Asp similarly enhances the affinity of divalent cation binding (for Mg^{2+}) in BIB. It is possible that block by external Ca^{2+} serves to increase the signal resolution that can be achieved with BIB channels, since the single channel conductance of BIB channels in

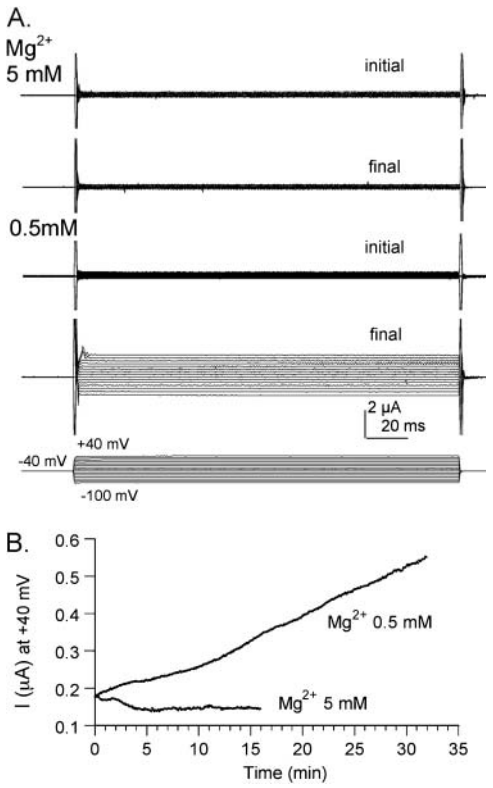

FIGURE 6 Comparison of the activation of BIB E71D current in standard and low Mg^{2+} salines. (*A*) Current traces measured at from +40 to −100 mV in 10-mV increments, from a single E71D-expressing oocyte. Currents are shown at the start of the recording period (*initial*; time 0) and after 15–30 min of maximal activation (*final*). Recordings were done first in 5 mM Mg^{2+} (*top two traces*); then after 3 h recovery in ND96 saline, the same oocyte was tested in 0.5 mM Mg^{2+} (*bottom two traces*). (*B*) Plot of the development of the current response, measured with repeated steps to +40 mV at 6-s intervals after electrode penetration at time 0 (same E71D-expressing oocyte as in *A*).

nominally Ca^{2+} free medium is very high (300 ± 30 pS; unpublished observations in Yanochko and Yool, 2002).

The signaling function of BIB in *Drosophila* nervous system development may be mediated by changes in membrane potential, enabled by BIB ion channel properties. Activation of cationic BIB channels would be expected to lead to depolarization of BIB-expressing cells. Of interest is the observation that in grasshopper embryos, differentiated neuroblasts show a negative membrane potential when compared with surrounding relatively depolarized nonneural cells, assuming the difference is not due to damage (Goodman and Spitzer, 1979). Although it is not known whether BIB contributes to the depolarization in nonneural grasshopper cells, this observation is consistent with results showing that BIB in *Drosophila* embryos is expressed in the plasma membrane of epidermal precursor cells, but not neuroblasts, and serves a necessary role in the lateral inhibition process (Doherty et al., 1997). Chronic endogenous block of the BIB conductance by external Ca^{2+} might be relevant for enhancing signal resolution or generating voltage-depen-

dence for the native process of neuronal cell fate determination; this physiological role remains to be defined.

The outward rectification of BIB currents in Ba^{2+} or Ca^{2+} salines suggests that unblocking occurs at depolarized potentials. The relative magnitude of rectification measured from the current-voltage relationships confirmed that wild-type BIB channels in Ca^{2+} and Ba^{2+} salines showed significantly more outward rectification than in Mg^{2+} saline, and that the novel block by Mg^{2+} in E71D channels was similarly voltage dependent. The decreased whole-cell conductance of E71D-expressing oocytes appears to be due to increased sensitivity to extracellular Mg^{2+} resulting in chronic block, as well as decreased plasma membrane expression.

Voltage-dependent block suggests that the site of block by divalent cations is located within the electrical field of the BIB ion channel, perhaps in the permeation pathway. Although the molecular structure of BIB remains to be determined, crystallographic analyses of the related channels, AQP1 and GlpF, provide a model for describing general features of candidate pore-lining regions in MIP channels. Both AQP1 and GlpF are homotetramers with individual pores for water or glycerol formed by loops B and E and located within the individual subunits of the tetramer. The limiting constrictions of the individual pores in each subunit are ~2.8 Å for AQP1 (Sui et al., 2001) and 3.4 × 3.8 Å for GlpF (Fu et al., 2000). In addition, a central cavity at the fourfold axis of symmetry, lined by transmembrane domains 2 and 5, has been hypothesized to serve as an ion channel in the subset of MIP channels that are ion-conducting (Yool and Weinstein, 2002), following a theme established for K^+ and CNG ion channels (Heginbotham et al., 1992). The putative central pore of AQP1 at the fourfold axis of symmetry has a limiting constriction estimated at <3 Å (Ren et al., 2001). At first glance, it would appear that ionic permeability studies do not match the predictions of crystal structures. The ionic radius of tetraethylammonium is ~5 Å, and its permeation through AQP1 and BIB channels (Yanochko and Yool, 2002; Yool et al., 1996) predicts that the limiting size of the ionic pore should be at least this large. However, it is important to recognize that crystal structure studies of AQP1 have been done in the absence of activating ligand and could reflect a closed, nonion-conducting state. Divalent cation binding in the central pore of GlpF, visualized by crystal structure analysis, supports the idea that this region might be a pathway for ion permeation in gated aquaporin ion channels (Fu et al., 2000). Another member of the aquaporin family, AQP6, has been described as an ion channel activated by mercury or acidic pH (Yasui et al., 1999). Although the AQP6 ion flux was suggested to occur through individual subunit pores (Hazama et al., 2002), the data available do not rule out involvement of the central pore. An amino acid sequence comparison of AQP6 and AQP1 indicates the residues that are critical for determining high specificity for water and creating a barrier for ions in the individual subunit pores of AQP1 (bovine sequence R197, H182, C191 and F58; Sui et al., 2001) also are present in AQP6, and thus the individual subunit pores would seem to be unlikely candidates for ion permeation.

A schematic diagram in Fig. 7 shows the positions of three negatively charged residues in a subunit of AQP1 that are equivalent to those mutated in BIB in our studies (BIB Glu^{71}, Asp^{253}, and Glu^{274} are homologous to bovine AQP1 Glu^{17}, Asp^{210}, and Asp^{230}, respectively). The Glu^{71} residue is also conserved in Glu^{17} of human AQP1 and Glu^{14} of GlpF. This Glu is thought to be buried in the protein and is not positioned clearly as a pore-lining residue for either the individual subunit pores or for the putative central pore (at least in closed state images). It is postulated to interact with a histidine residue (H^{69}) near M2 in human AQP1 (equivalent to H^{71} in bovine AQP1; Fig. 7) and to be critical in maintaining structural integrity of the channel protein (Ren et al., 2001). Our data support a crucial role for BIB Glu^{71} in determination of ion channel properties, either directly by contributing to a binding site that becomes available with channel opening or indirectly by supporting structures that in turn establish ion conductance properties of the channel. It will be interesting in future experiments to determine whether any of the nonconducting Glu^{71} mutants are useful as dominant negative constructs for studying the roles of BIB in developmental signaling in native tissues. Further work is needed to analyze the physiological role of BIB ion channel activation in the process of early de-

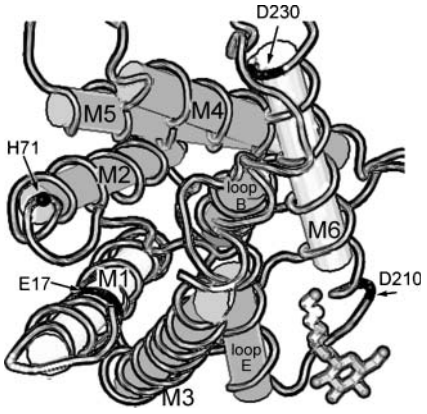

FIGURE 7 Schematic diagram of a subunit of bovine Aquaporin-1, viewed from the cytoplasmic side. M1–M6 are membrane-spanning domains; loops B and E line the water pore within the individual subunit. The central cavity (putative ion pore) of the tetramer is lined by M2 and M5. Notations are Glu (*E*), Asp (*D*), and His (*H*). E^{17} in M2 and D^{210} and D^{230} near M6 (*black fill*) are homologous to the residues mutated in BIB (E^{71}, D^{253}, and E^{274}). H^{71} (●) is postulated to interact with E^{17} in AQP1. The diagram is based on crystal structure data for bovine AQP1 (Sui et al., 2001) from the National Center for Biotechnology Information (NCBI) Molecular Modeling Database. File: MMDB 18789; PDB 1J4N; analyzed with Cn3D 3.0; available from http://www.ncbi.nlm.nih.gov. Structural similarities between BIB and AQP1 seem plausible but have not yet been demonstrated.

velopment and cell fate determination in the nervous system and the potentially interesting role of block by endogenous divalent cations such as Ca^{2+} in defining the properties of transmembrane signaling between developing cells. Big Brain is another example of the intriguing diversity of functions that are being discovered for ion channels in the MIP family.

We thank Dr. Jill Steidl for assistance with data analysis, Drs. W. Daniel Stamer and Jeremy Richman for helpful discussions regarding site-directed mutagenesis strategies, and Amy Marble for technical support.

This work was supported by National Institutes of Health RO1 GM 59986 (A.J.Y.), National Institutes of Health Training Grant T32 NS-07363, and University of Arizona Michael Cusanovich Dean's Research Fellowship (G.M.Y.).

REFERENCES

Anthony, T. L., H. L. Brooks, D. Boassa, S. Leonov, G. M. Yanochko, J. W. Regan, and A. J. Yool. 2000. Cloned human aquaporin-1 is a cyclic GMP-gated ion channel. *Mol. Pharmacol.* 57:576–588.

Doherty, D., L. Y. Jan, and Y. N. Jan. 1997. The Drosophila neurogenic gene big brain, which encodes a membrane-associated protein, acts cell autonomously and can act synergistically with Notch and Delta. *Development.* 124:3881–3893.

Fu, D., A. Libson, L. J. Miercke, C. Weitzman, P. Nollert, J. Krucinski, and R. M. Stroud. 2000. Structure of a glycerol-conducting channel and the basis for its selectivity. *Science.* 290:481–486.

Goodman, C. S., and N. C. Spitzer. 1979. Embryonic development of identified neurones: differentiation from neuroblast to neurone. *Nature.* 280:208–214.

Hazama, A., D. Kozono, W. B. Guggino, P. Agre, and M. Yasui. 2002. Ion permeation of AQP6 water channel protein. Single channel recordings after Hg2+ activation. *J. Biol. Chem.* 277:29224–29230.

Heginbotham, L., T. Abramson, and R. MacKinnon. 1992. A functional connection between the pores of distantly related ion channels as revealed by mutant K+ channels. *Science.* 258:1152–1155.

Kaupp, U. B., and R. Seifert. 2002. Cyclic nucleotide-gated ion channels. *Physiol. Rev.* 82:769–824.

Lehmann, R., F. Jimenez, and U. Dietrich. 1983. On the phenotype and development of mutants of early neurogenesis in *Drosophila* melanogaster. *Roux. Arch. Dev. Biol.* 192:62–74.

MacDonald, J. F., and L. M. Nowak. 1990. Mechanisms of blockade of excitatory amino acid receptor channels. *Trends Pharmacol. Sci.* 11: 167–172.

Nichols, C. G., and A. N. Lopatin. 1997. Inward rectifier potassium channels. *Annu. Rev. Physiol.* 59:171–191.

Park, C. S., and R. MacKinnon. 1995. Divalent cation selectivity in a cyclic nucleotide-gated ion channel. *Biochemistry.* 34:13328–13333.

Preston, G. M., T. P. Carroll, W. B. Guggino, and P. Agre. 1992. Appearance of water channels in Xenopus oocytes expressing red cell CHIP28 protein. *Science.* 256:385–387.

Rao, Y., R. Bodmer, L. Y. Jan, and Y. N. Jan. 1992. The big brain gene of *Drosophila* functions to control the number of neuronal precursors in the peripheral nervous system. *Development.* 116:31–40.

Rao, Y., L. Y. Jan, and Y. N. Jan. 1990. Similarity of the product of the *Drosophila* neurogenic gene big brain to transmembrane channel proteins. *Nature.* 345:163–167.

Reizer, J., A. Reizer, and M. H. Saier, Jr. 1993. The MIP family of integral membrane channel proteins: sequence comparisons, evolutionary relationships, reconstructed pathway of evolution, and proposed functional differentiation of the two repeated halves of the proteins. *Crit. Rev. Biochem. Mol. Biol.* 28:235–257.

Ren, G., V. S. Reddy, A. Cheng, P. Melnyk, and A. K. Mitra. 2001. Visualization of a water-selective pore by electron crystallography in vitreous ice. *Proc. Natl. Acad. Sci. USA.* 98:1398–1403.

Stern, J. H., H. Knutsson, and P. R. MacLeish. 1987. Divalent cations directly affect the conductance of excised patches of rod photoreceptor membrane. *Science.* 236:1674–1678.

Sui, H., B. G. Han, J. K. Lee, P. Walian, and B. K. Jap. 2001. Structural basis of water-specific transport through the AQP1 water channel. *Nature.* 414:872–878.

Yanochko, G. M., and A. J. Yool. 2002. Regulated cationic channel function in Xenopus oocytes expressing Drosophila big brain. *J. Neurosci.* 22:2530–2540.

Yasui, M., A. Hazama, T. H. Kwon, S. Nielsen, W. B. Guggino, and P. Agre. 1999. Rapid gating and anion permeability of an intracellular aquaporin. *Nature.* 402:184–187.

Yool, A. J., W. D. Stamer, and J. W. Regan. 1996. Forskolin stimulation of water and cation permeability in aquaporin 1 water channels. *Science.* 273:1216–1218.

Yool, A. J., and A. M. Weinstein. 2002. New roles for old holes: ion channel function in aquaporin-1. *News Physiol. Sci.* 17:68–72.

Zimmerman, A. L., and D. A. Baylor. 1992. Cation interactions within the cyclic GMP-activated channel of retinal rods from the tiger salamander. *J. Physiol.* 449:759–783.